

Ada-KV: Optimizing KV Cache Eviction by Adaptive Budget Allocation for Efficient LLM Inference

Yuan Feng^{1,3,†}, Junlin Lv^{1,3,†}, Yukun Cao^{1,3}, Xike Xie^{2,3,*}, and S. Kevin Zhou^{2,3}

¹School of Computer Science, University of Science and Technology of China (USTC), China

²School of Biomedical Engineering, USTC, China

³Data Darkness Lab, MIRACLE Center, Suzhou Institute for Advanced Research, USTC, China
{yfung,junlinlv,ykcho}@mail.ustc.edu.cn, xkxie@ustc.edu.cn, s.kevin.zhou@gmail.com

Abstract

Large Language Models have excelled in various fields but encounter efficiency limitations due to the substantial Key-Value (KV) cache required for long-sequence inference. Recent efforts try to evict non-critical cache elements during runtime, thereby reducing cache size within given memory budgets while preserving generation quality. Our reexamination of foundational principles reveals that prevailing methods aim to minimize an upper bound of eviction loss, quantified as the L1 distance between the pre- and post-eviction outputs of multi-head self-attention mechanisms. Moreover, our analysis indicates that the common practices of uniformly assigning budgets across different attention heads during cache eviction hinder their budget utilization, negatively impacting generation quality. In light of these findings, we propose a simple yet effective adaptive budget allocation algorithm. This algorithm not only optimizes the loss upper bound in theory but also reduces the eviction loss in practice by aligning with the intrinsic patterns of self-attention mechanisms. Integrating this algorithm into two advanced methods, we develop Ada-SnapKV and Ada-Pyramid. Extensive evaluations on 16 datasets and the Needle-in-a-Haystack test confirm that they both significantly boost performance across various tasks.

1 Introduction

Autoregressive Large language models (LLMs) have achieved significant success and are widely utilized across diverse natural language processing applications, including dialogue systems (Yi et al. 2024), document summarization (Laban et al. 2023), and code generation (Gu 2023). The widespread deployments have propelled the development of their capacities to process extended sequences. For instance, GPT-4 supports sequences up to 129K (Achiam et al. 2023), Claude3 up to 200K (Anthropic 2024), and Gemini-Pro-1.5 (Reid et al. 2024) up to 1M tokens. However, transformer-based LLMs pose significant efficiency challenges while processing long-sequence inputs.

Specifically, the inference process of LLMs consists of two stages: *prefilling* and *decoding*. During prefilling, LLMs compute and store all Key-Value (KV) cache pairs for the input tokens from the prompt. In the subsequent decoding phase, LLMs autoregressively generate each output token

using the most recent token and all previous KV cache pairs. This stage continues until the maximum designated length is reached or it is actively stopped. However, while dealing with the long-sequence inputs, the size of the generated KV cache significantly increases, easily exceeding the model’s parameter size (Sun et al. 2024). This escalation leads to substantial storage challenges during both the prefilling and decoding stages. Additionally, during the decoding phase, each autoregressive step requires extensive KV cache I/O, which incurs significant I/O latency. This latency now exceeds the time required for computation and becomes the primary bottleneck in decoding speed (Tang et al. 2024; Dao et al. 2022). Consequently, the extensive KV cache associated with long sequences poses significant efficiency challenges for the inference process.

In response to the challenges posed by large KV cache size, a range of KV cache eviction methods have been developed, as referenced in recent literature (Zhang et al. 2024b; Xiao et al. 2023; Ge et al. 2023; Yang et al. 2024; Zhang et al. 2024a; Li et al. 2024). As shown in Figure 1, these methods discard most non-critical cache pairs after the prefilling stage of each layer in LLMs. Therefore, by tailoring the cache sizes to specified storage budgets, they not only reduce the storage burden but also boost the decoding speed while maintaining the post-eviction generation quality. These eviction methods are designed with plug-and-play capabilities, allowing for straightforward integration into any LLM setup without the need for fine-tuning. They typically utilize various strategies to selectively evict the majority of KV cache pairs. The latest leading methods (Li et al. 2024; Yang et al. 2024; Zhang et al. 2024a), employ a Top-K based selection scheme based on attention weights. These approaches effectively distinguish between critical and non-critical cache pairs, deciding which to retain and which to evict. Despite these advancements, the challenge of minimizing quality loss while employing these eviction methods remains an unresolved issue in the field.

Our study begins by reexamining the underlying principles of eviction methods from a theoretical perspective. We reveal that Top-K based methods aim to minimize an upper bound of eviction loss, quantified as the L1 distance between the pre- and post-eviction outputs of self-attention mechanisms. Moreover, We find the common practice of uniformly assigning budgets across different attention heads leads to

[†]Equal Contribution *Corresponding Author

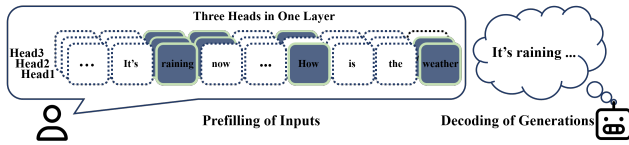
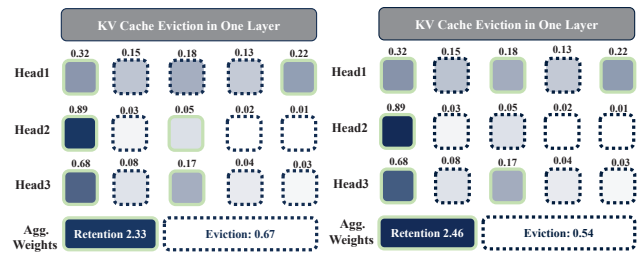


Figure 1: Cache Eviction Framework. Cache Eviction removes a large number of non-essential tokens, marked by dashed borders, immediately after the prefilling stage of each layer. This process substantially reduces storage requirements and accelerates decoding, while preserving the quality of post-eviction generations.

a misallocation of budgets, thus limiting budget utilization. Based on these insights, we propose a simple yet effective adaptive allocation algorithm. As an illustrative example shown in Figure 2, it effectively improves budget utilization by dynamically allocating the budget across different attention heads within the same layer based on their concentration degrees, thereby enhancing the quality of post-eviction generation. We substantiate the advantages of adaptive allocation both theoretically and empirically. Theoretically, as detailed in Section 3.4, the adaptive allocation reduces the upper bound of eviction loss compared to the current uniform allocation. Empirically, as detailed in Section 3.5, the alignment of the adaptive allocation with inherent varied degrees in attention concentration among the heads within self-attention mechanisms effectively reduces eviction loss in practice.

By integrating this adaptive budget allocation algorithm into two advanced methods (Li et al. 2024; Yang et al. 2024; Zhang et al. 2024a), we develop two adaptive eviction methods: Ada-SnapKV and Ada-Pyramid, respectively. Extensive evaluations across 16 datasets, spanning various tasks in LongBench (Bai et al. 2023), demonstrate that both Ada-SnapKV and Ada-Pyramid significantly improve the generation quality. Additionally, the Needle-in-a-Haystack test, a widely used evaluation method, further confirms that adaptive allocation enhances in-context retrieval ability. The main contributions are summarized as follows:

- **Reexamination of Cache Eviction Principle:** We reveal the principles of cache eviction methods that aim to minimize an upper bound of eviction loss, quantified as the L1 distance between the pre- and post-eviction attention outputs.
- **Identifying and Addressing Limitations in Budget Allocations:** We pinpoint the inefficiency of existing uniform budget allocation across heads. To address this, we introduce an adaptive allocation algorithm that not only optimizes the upper bound in theory but also reduces the eviction loss in practice.
- **Developments of Adaptive Eviction Methods:** By integrating adaptive allocation, we develop two novel methods: Ada-SnapKV and Ada-Pyramid. These methods both significantly improve the post-eviction generation quality in the extensive evaluations.
- **Innovative Direction to Enhance Cache Eviction:** Our research pioneers a new direction by adaptively allocating budgets based on unique characteristics among heads



(a) Uniform Allocation (b) Adaptive Allocation

Figure 2: An Illustrative Example. This example features a five KV cache pairs with associated attention weights across three heads. Adaptive allocation, through reallocating budgets from the concentrated Head2 to the dispersed Head1, increases the aggregated weights of retained KV cache pairs from 2.33 to 2.46, which correlates to a reduced eviction loss in Section 3.4 and 3.5.

to optimize cache eviction. This innovation, guided by our theoretical analysis of the upper bounds of eviction loss, seeks significant further development in this field.

2 Related Works

In the context of long-sequence inference, the vast scale of the KV cache pairs leads to a memory-bound situation, causing significant storage and I/O latency costs (Wang and Chen 2023). Some studies employ efficient memory management strategies that reduce I/O time without altering the size of the KV Cache, such as Page Attention (Kwon et al. 2023) and Flash Attention (Dao et al. 2022). These studies are orthogonal to our work and we incorporate the Flash Attention technique in our implementation to achieve efficient computation. Some works, called KV cache quantization, reduce the size of cache pairs by lowering the precision of individual entries. However, its compression ratio is inherently limited—ideally, quantization from 16-bits to 1-bit achieves a theoretical limit of 6.25% compression but results in catastrophic quality degradation. However, cache eviction methods could compress the KV Cache to any given small budget, like less than 1% of the original size while still maintaining certain generation quality. Moreover, the techniques of quantization and eviction are orthogonal, suggesting potential for further combined optimization in the future. Another work (Tang et al. 2024) attempts to reduce I/O overhead by only recalling KV cache pairs relevant to the current query for computation. However, it is constrained by substantial memory overheads, making deployment on GPUs with limited storage capacities challenging.

Recently, KV cache eviction methods have gained attention and rapid development due to their flexible compression ratios given any storage budgets and the advantage of being plug-and-play without the need for fine-tuning. Earlier StreamingLLM (Xiao et al. 2023) simply maintains the cache of 4 initial and the recent tokens, discarding all others to adapt to long sequence inference. FastGen (Ge et al. 2023) searches and combines multiple strategies, like maintaining the cache of special tokens, punctuation tokens, and recent tokens, based on the characteristics of attention heads.

H2O (2024b) has developed an eviction algorithm that utilizes query states of all tokens to identify important KV pairs based on the Heavy Hitter method. The most recent SnapKV (Li et al. 2024) identifies important KV cache pairs using query states of several tokens within a recent window, evicting the less important ones. This method effectively mitigates the quality degradation in cache eviction. The Pyramid (Yang et al. 2024; Zhang et al. 2024a) further adjusts the budget allocation across different layers in SnapKV, improving the generation quality in small-budget scenarios. However, to our best knowledge, current eviction methods have never tried to adaptively distribute the total budget across different heads. Building on theoretical analysis and observations of inherent attention patterns in LLM heads, we identify and demonstrate the necessity for adaptive budget allocation in cache eviction.

3 Framework

3.1 Overview

In this section, we reexamine how the existing cache eviction strategies retain essential information in the past KV cache from a theoretical perspective. Inspired by theoretical findings, we propose a simple yet effective algorithm for adaptive budget allocation, which is proven to be better than the previous uniform allocation method in cache eviction procedures, both theoretically and practically. Upon further integrating this algorithm into two leading existing methods, we have developed two adaptive cache eviction techniques: Ada-SnapKV and Ada-Pyramid. The key findings and insights are as below:

- **How do the eviction strategies maintain generation quality despite discarding substantial KV cache?** Theorem 2 formalizes an upper bound of the eviction loss by using the L1 distance between the pre- and post-eviction outputs and Theorem 3 demonstrates that Top-K based eviction strategies aim to minimize this upper bound.
- **Why is adaptive budget allocation better from the theoretical perspective?** Theorem 4 demonstrates that the upper bound of eviction loss under adaptive allocation maintains at or below that under previous uniform allocation in the cache eviction procedure. Thus it implies that the adaptive allocation is better in theory.
- **Why is adaptive budget allocation better from the empirical perspective?** As shown in Figure 3 and 4, we identify that the inherent disparities in attention concentration across different heads reliably translate theoretical advantages into practical results, leading to consistent reductions of eviction loss in practice.

3.2 Preliminary

We begin by providing a formal description of the computational processes involving Multi-head Attention and KV cache in a single-layer of LLMs to alleviate the burden of notation. LLMs are characterized by their autoregressive generation mode, where each step involves using the last token to predict the next token. Define $X \in \mathbb{R}^{n \times d}$ as the embedding matrix of all tokens in sequence, and $x \in \mathbb{R}^{1 \times d}$ as the

last token used as input at the current timestep. To clarify the subsequent theoretical exposition, we adopt the notation system from (Liu et al. 2023) under the assumption of h attention heads in one layer. The transformation matrices for each head $i \in [h]$, $W_i^Q, W_i^K, W_i^V \in \mathbb{R}^{d \times d_h}$, map token embeddings to their respective Query, Key, and Value and the final output matrix $W_i^O \in \mathbb{R}^{d_h \times d}$ transform the intermediate result to the output hidden states. At each timestep, the previous KV cache pairs on head i have been initialized as:

$$K_i = XW_i^K, V_i = XW_i^V \quad (1)$$

Then, the input token x is mapped to its corresponding query, key, value for each head, and the previous KV cache is updated accordingly:

$$q_i = xW_i^Q, k_i = xW_i^K, v_i = xW_i^V \quad (2)$$

$$K_i = [K_i : k_i], V_i = [V_i : v_i] \quad (3)$$

Finally the final output $o \in \mathbb{R}^{1 \times d}$ is computed as follow:

$$o = \sum_{i \in [h]} A_i V_i W_i^O \quad (4)$$

where $A_i \in \mathbb{R}^{1 \times n}$ is the attention weight calculated by¹:

$$A_i = \text{softmax}(q_i K_i^T) \quad (5)$$

3.3 Reexamining the Principle of Cache Eviction

Cache eviction is dedicated to reducing the size of KV cache to fit within a constrained budget by evicting non-critical cache pairs strategically. Eviction masks $\{\mathcal{M}_i \in \mathbb{R}^{1 \times n}\}$ can be employed to simulate the post-eviction output o' of self-attention mechanism during the generation process:

$$o' = \sum_{i \in [h]} A'_i V_i W_i^O \text{ where } A'_i = \text{softmax}(q_i K_i^T + \mathcal{M}_i) \quad (6)$$

where each element \mathcal{M}_i^j ² in mask \mathcal{M}_i indicates that whether the j th $\in [n]$ KV cache pair has been evicted in $K_i, V_i \in \mathbb{R}^{n \times d_h}$ on each head i :

$$\mathcal{M}_i^j = \begin{cases} 0 & \text{if the } j\text{th cache pair on head } i \text{ is retained} \\ -\infty & \text{otherwise the } j\text{th cache pair on head } i \text{ is evicted} \end{cases}$$

$$\text{given budget allocation } \{B_i\} \text{ s.t. } \sum_{i \in [h]} B_i = B$$

Thus, the budget B_i for head i corresponds to the number of zero elements in \mathcal{M}_i . Theorem 1 further simplifies the output o' by eliminating the softmax function. A detailed proof is provided in Appendix A.1.

¹The scaling factor $\sqrt{d_h}$ is omitted for simplification.

²Given the first dimension of \mathcal{M}_i is 1, \mathcal{M}_i^j is used to simplify the notation for $\mathcal{M}_i(1, j)$. Similarly, A_i^j is in the same manner.

Theorem 1. *The post-eviction output o' can rewrite as:*

$$o' = \sum_{i \in [h]} \frac{A_i \odot \mathcal{N}_i}{\|A_i \odot \mathcal{N}_i\|_1} V_i W_i^O \quad (7)$$

$$\text{where } \mathcal{N}_i^j = \begin{cases} 1 & \text{if } K_i^j \text{ and } V_i^j \text{ are retained} \\ 0 & \text{otherwise, evict } K_i^j \text{ and } V_i^j \end{cases}$$

and \odot indicates element-wise multiplication

$$\text{given budget allocation } \{B_i\} \text{ s.t. } \sum_{i \in [h]} B_i = B$$

The reduction in generation quality during cache eviction stems from changes in the attention output. Thus, we quantify the eviction loss as the L1 distance between the pre- and post-eviction outputs of self-attention mechanisms:

$$\text{Eviction Loss} = \|o - o'\|_1 \quad (8)$$

Utilizing the row norm of matrix, we derive an upper bound D for the Eviction Loss in Theorem 2. For a detailed proof, refer to Appendix A.2.

Theorem 2. *The eviction loss caused by cache eviction can be bounded by D as follows:*

$$\text{Eviction Loss} \leq D = 2hC - 2C \sum_{i \in [h]} \sum_{\text{retained } j} A_i^j \quad (9)$$

$$\text{given budget allocation } \{B_i\} \text{ s.t. } \sum_{i \in [h]} B_i = B$$

where $C = \text{Max} \{\|V_i W_i^O\|_\infty\}$ is the max value in the row norms of Matrices $\{V_i W_i^O\}$ among all heads.

Cache eviction strategies typically presuppose the stability of critical cache pairs (Zhang et al. 2024b; Li et al. 2024; Yang et al. 2024; Zhang et al. 2024a), thereby facilitating cache eviction during the autoregressive generation process. Consequently, the advanced strategies leverage query states from several recent tokens to calculate attention weights with all past cache pairs, which, in conjunction with Top-K selections, approximate the identification of cache pairs critical in subsequent generations. For simplicity, we assume that the eviction procedure relies solely on a single query state q_i associated with the last token x for critical cache detection. As shown in Algorithm 1, the core idea of current leading eviction strategies based on Top-K selections is only to retain cache pairs corresponding to B_i highest weights $A_i^j \in \text{Top-K}(A_i, B_i)$, while evicting those considered non-essential. Obviously, given the budget allocation $\{B_i\}$ the Top-K based eviction strategies maximize the aggregated weights as follows:

$$\text{Top-K Eviction} = \arg \max_{\text{strategy}} \sum_{i \in [h]} \sum_{\text{retained } j} A_i^j. \quad (10)$$

$$\text{given budget allocation } \{B_i\} \text{ s.t. } \sum_{i \in [h]} B_i = B$$

Therefore, we establish Theorem 3, which demonstrates that the principle of Top-K based eviction aims to minimize an upper bound D .

Algorithm 1: Eviction Based on Top-K Selection

Input: Allocation $\{B_i\}$, KV Cache $\{K_i, V_i\}$, Weights $\{A_i\}$

Output: Compressed cache $\{\hat{K}_i, \hat{V}_i\}$

```

1: for  $i \leftarrow 1$  to  $h$  do
2:   initialize empty cache  $\hat{K}_i, \hat{V}_i$  for head  $i$ 
3:   for  $j \leftarrow 1$  to  $n$  do
4:     if  $A_i^j \in \text{Top-K}(A_i, B_i)$  then
5:       retain and append cache pair  $K_i^j, V_i^j$  to  $\hat{K}_i, \hat{V}_i$ 
6:     else
7:       evict cache pair  $K_i^j, V_i^j$ 
8:     end if
9:   end for
10: end for
11: return compressed cache  $\{\hat{K}_i, \hat{V}_i\}$ 

```

Theorem 3. *Given a budget allocation result $\{B_i\}$, the principle of eviction strategies based on Top-K selections is to minimize the upper bound D of eviction loss.*

$$\text{Top-K Eviction} = \arg \min_{\text{strategy}} D \quad (11)$$

$$\text{given budget allocation } \{B_i\} \text{ s.t. } \sum_{i \in [h]} B_i = B$$

3.4 Adaptive vs. Uniform: Theoretical Perspective

In existing studies on cache eviction, the budget B is uniformly assigned across all heads within a layer: specifically, $B_i = B/h$. Consequently, the upper bound of eviction loss D is modified to D' under uniform allocation:

$$D' = 2hC - 2C \sum_{i \in [h]} \sum_{\substack{j \in [n] \\ A_i^j \in \text{Top-K}(A_i, B_i)}} A_i^j \quad (12)$$

$$\text{given uniform budget allocation } \{B_i = B/h\}$$

In contrast, we suggest adaptive allocation of the overall budget among heads and introduce a simple yet effective budget allocation algorithm that dynamically distributes the total budget B based on the attention weights A_i across heads, with the allocated results denoted as $\{B_1^*, B_2^*, \dots, B_h^*\}$ subject to $\sum_{i \in [h]} B_i^* = B$. As shown in Algorithm 2, it firstly selects the B largest attention weights from all heads within one layer. Based on the times each head is selected during the above procedure, different budgets B_i^* are allocated to each head. Under this adaptive allocation, the upper bound of eviction loss D is modified to D'' :

$$D'' = 2hC - 2C \sum_{i \in [h]} \sum_{\substack{j \in [n] \\ A_i^j \in \text{Top-K}(A_i, B_i^*)}} A_i^j \quad (13)$$

$$\text{given adaptive budget allocation } \{B_i = B_i^*\}$$

Algorithm 2: Adaptive Budget Allocation

Input: Total Budget B , Attention Weights in h heads $\{A_i \in \mathbb{R}^{1 \times n}\}$;

Output: Allocated Budgets of h heads $\{B_i^*\}$;

- 1: Concatenate across heads $A = \text{Cat}(\{A_i\}, \text{dim}=1)$
 - 2: Create head indicator $I = [1 \dots 1 : \dots : h \dots h]$ with each index $\{i\}$ repeat n times
 - 3: Identify top indices $T = \text{Top-K}(A, B)$.indices
 - 4: Select the corresponding head indicator $I^* = I[T]$
 - 5: Count frequencies of each i in I^* to determine $\{B_i^*\}$
 - 6: **return** Allocated Results of h heads $\{B_i^*\}$
-

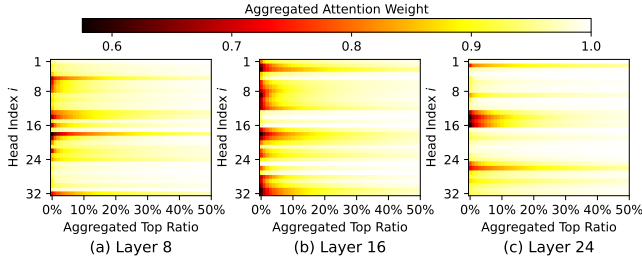


Figure 3: Disparities in Attention Concentration Across Heads. (Mistral-instruct-v0.2 on the first sample of the Qasper, a single-doc QA dataset in LongBench) We aggregate different proportions of the top attention weights, $\sum_{\text{retained } j} A_i^j$, to analyze attention concentration in different head i . Most concentrated heads require a small cache proportion, e.g., 5%, to aggregate weights close to 1, whereas other dispersed heads need significantly larger proportions, such as 50%.

Theorem 4. *The upper bound D'' of eviction loss with adaptive budget allocation consistently remains at or below the upper bound D' associated with uniform allocation.*

$$D'' \leq D' \quad (14)$$

According to Theorem 4, our adaptive allocation algorithm achieves equal or smaller eviction loss upper bound compared to the previous uniform allocation, thereby offering theoretical advantages. The detailed proof can be found in Appendix A.3.

3.5 Adaptive vs. Uniform: Empirical Perspective

According to Theorem 4, the upper bound of eviction loss of adaptive allocation is equal to or less than that of the prevailing uniform allocation. We further demonstrate different attention heads within each layer of LLMs exhibit significant disparities in the degrees of attention concentration, which effectively translates this theoretical advantage of a reduced upper bound into practical reductions in eviction loss.

For visualization in Figure 3 (a), most concentrated heads in Layer 8 like head 1 require only 1% of the original cache budget to effectively retain the aggregated weights $\sum_{\text{retained } j} A_i^j$ of 0.95. Conversely, other heads like head 18 require nearly 50% proportion to near 0.95. This characteristic is closely related to the upper bound D of eviction

Algorithm 3: Ada-SnapKV/Ada-Pyramid in One Layer

Input: Overall budget B , Past cache $\{K_i, V_i\}$, Tokens in the recent window $X^{rec} \in \mathbb{R}^{\text{win} \times d}$

Output: Compressed cache $\{\hat{K}_i, \hat{V}_i\}$

- 1: **for** $i \leftarrow 1$ to h **do**
 - 2: $Q_i^{rec} = X^{rec} W_i^Q$
 - 3: $\bar{A}_i = \text{softmax}(Q_i^{rec} K_i^T)$
 - 4: $\bar{A}_i = \bar{A}_i.\text{maxpooling}(\text{dim} = 1).\text{mean}(\text{dim} = 0)$
 - 5: **end for**
 - 6: get $\{B_i^*\}$ by invoking Algorithm 2($B, \{\bar{A}_i\}$)
 - 7: $\{B_i^*\} = \alpha \times \{B_i^*\} + (1 - \alpha) \times \frac{B}{h}$
 - 8: $\{\hat{K}_i, \hat{V}_i\} = \text{Algorithm 1}(\{B_i^*\}, \{K_i, V_i\}, \{\bar{A}_i\})$
 - 9: **return** compressed cache $\{\hat{K}_i, \hat{V}_i\}$
-

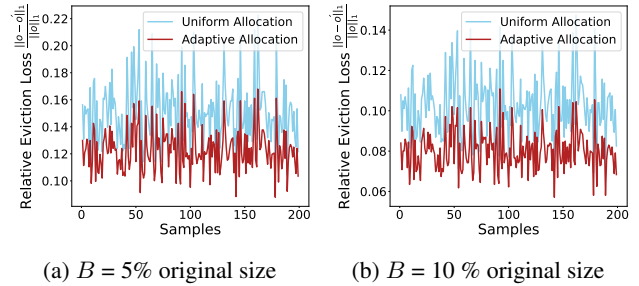


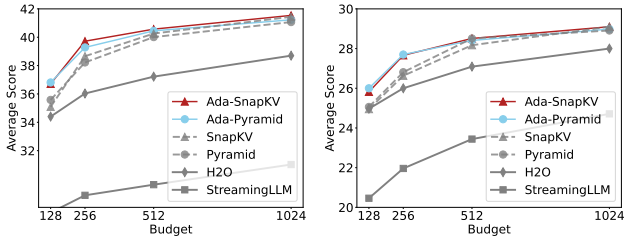
Figure 4: Comparison of Eviction Losses. (Using Mistral-7B-instruct-v0.2 on 200 samples from the Qasper Dataset) Cache eviction is implemented under Uniform and Adaptive allocation strategies respectively, compressing the original cache size to 5% and 10%. The adaptive version consistently yields a lower average relative eviction loss $\frac{\|o-o'\|_1}{\|o\|_1}$ across all layers on different samples compared to the prevailing uniform allocation.

loss, as detailed in Theorem 3. Under such circumstances, the previous uniform allocation encounters a budget utilization dilemma, as an illustrative example in Figure 2: it must either endure substantial eviction losses in dispersed heads or waste excessive and unwarranted budgets on heads with concentrated attention. This significantly undermines the trade-off performance between the total budget and generation quality in the cache eviction. In contrast, the adaptive allocation algorithm assigns large budgets to dispersed heads, while controlling the budget sizes for other heads, effectively maintaining the overall size and mitigating the decline in generation quality. In Figure 4, we show the averaged relative eviction loss in all layers, $\frac{\|o-o'\|_1}{\|o\|_1}$, with uniform and adaptive allocations separately. Results show that the adaptive allocation consistently reduces eviction losses across all 200 samples in the Qasper dataset. This indicates that adaptively allocating budgets among different heads enhances the budget utilization significantly, thereby reducing the output eviction loss.

3.6 Implementation

The current two leading eviction strategies, SnapKV and Pyramid, both utilize the several tokens $X^{rec} \in \mathbb{R}^{win*d}$ from a recent window (typically window size is 32) to identify and evict the less important cache pairs. SnapKV excels at scenarios with large budgets, while Pyramid is more effective in smaller budgets. The key distinction lies in how Pyramid and SnapKV allocate budgets within different layers in LLMs. Pyramid suggests that information aggregation among layers takes a pyramidal form, thereby allocating a larger budget to shallower layers and progressively reducing it in deeper layers through pre-set hyper-parameters. In contrast, SnapKV distributes the budget uniformly across all layers. Nonetheless, same as other eviction methods, they both allocate the budget uniformly among all heads within a single layer. Thus, for a specific layer with a overall budget of B , their eviction algorithms are the same.

We incorporate our adaptive allocation algorithm into both of them, resulting in the creation of two novel adaptive strategies: Ada-SnapKV and Ada-Pyramid, respectively. As shown in Algorithm 3³, the adaptive budget allocation can be seamlessly integrated into any eviction strategy by invoking the adaptive allocation Algorithm 2 before eviction process in each layer. Both of Ada-SnapKV and Ada-Pyramid utilize a max pooling layer to facilitate cache selection following the previous SnapKV (Li et al. 2024) and Pyramid (Zhang et al. 2024a). Besides, a hyper-parameter α in line 6, set by default to 0.5, prevents assigning tiny budgets to highly concentrated heads, thereby enhancing fault tolerance of critical cache detection. Additionally, we incorporate the Flash Attention (Kwon et al. 2023) technique to support efficient computation of variable-length head caches, with the computational efficiency evaluations provided in Appendix A.4.



(a) Mistral-7B-Instruct-v0.2 (b) LWM-Text-Chat-1M

Figure 5: Average Score Among 16 Datasets

4 Experiments

4.1 Settings

Datasets Firstly, we carry out an comprehensive evaluation using 16 datasets, covering domains of single-document QA (Kočiský et al. 2018; Dasigi et al. 2021), multi-document QA (Yang et al. 2018; Ho et al. 2020; Trivedi et al. 2022), summarization (Huang et al. 2021; Zhong et al. 2021; Fabbri et al. 2019), few-shot learning (Joshi et al.

³Algorithm 3 describes the process serially for simplicity, but eviction operations can be parallelized easily in practice.

2017; Gliwa et al. 2019; Li and Roth 2002), Synthetic (Bai et al. 2023), and code generation (Guo et al. 2023; Liu, Xu, and McAuley 2023), within LongBench (Bai et al. 2023), a benchmark for evaluating multi-task performance with long-sequence inputs. These datasets feature varying average input lengths from 1,235 to 18,409 tokens, necessitating substantial KV cache size during generation, thereby rendering them suitable for evaluating KV cache eviction strategies. Each dataset is assessed using LongBench-recommended metrics, with quality scores up to 100. Detailed dataset information is provided in Appendix A.6. We also utilize the widely-used 'Needle-in-a-Haystack' test, where key information is randomly inserted into long texts to create prompts. This test evaluates whether LLMs can extract this key information from extensive texts, specifically examining the impact of proposed adaptive allocation on the models' fundamental long context retrieval abilities.

Baselines We conduct a comparative analysis between our newly proposed methods, *Ada-SnapKV* and *Ada-Pyramid*, and the previously established *SnapKV* and *Pyramid*, acknowledged as two leading approaches under varying scenarios. Additionally, we assess these methods against other earlier eviction strategies, including *StreamingLLM* and *H2O*. *StreamingLLM* is designed to handle long-sequence inputs by retaining caches of several initial tokens and others in a recent window. And *H2O* compresses cache size by employing attention weight-based detection of Heavy Hitters based on all queries and key states. In all experiments, the hyper-parameter α in Algorithm 2 is set to 0.5. Both *Ada-SnapKV* and *Ada-Pyramid*, as well as *SnapKV* and *Pyramid*, utilize the same configuration settings as described in (Li et al. 2024), ensuring comparability with a recent window size of 32 and a maximum pooling kernel size of 7. Parameters for *StreamingLLM* and *H2O* conform to the default settings reported in the literature (Zhang et al. 2024b; Xiao et al. 2023).

Base Models In the experiments, we employ two open-source base models: Mistral-7B-instruct-v0.2 (Jiang et al. 2023) and LWM-Text-Chat-1M (Liu et al. 2024). The Mistral 7B model features a context length of 32K and has been adopted as the primary model in related studies (Li et al. 2024; Zhang et al. 2024a) due to its moderate parameter size and remarkable capability for long text tasks. Meanwhile, LWM 7B model stands as the state of the art with its 1M context length, facilitating performance evaluations for the Needle-in-a-Haystack test under extreme context lengths.

4.2 Evaluations Among 16 Datasets

We assess all eviction strategies using cache budget $B \in \{128 \times h, 256 \times h, 512 \times h, 1024 \times h\}$ for each layer. Detailed results for each dataset on the Mistral model are provided in Table 1, while other results for the LWM model are placed in Appendix A.5 due to space constraints. To demonstrate the efficacy of adaptive allocation, we take a budget $B = 128h$ as an example presented in Table 1. After integrating the adaptive allocation algorithm, *Ada-SnapKV* enhances the quality scores in 15 out of 16 datasets compared to the original SnapKV, increasing the average score from

	Single-Doc. QA			Multi-Doc. QA			Summarization			Few-shot Learning			Synthetic		Code		Ave. Score
	NrtvQA	Qasper	MF-en	HotpotQA	2WikiMQA	Musique	GovReport	QMSum	MultiNews	TREC	TriviaQA	SAMSum	PCount	PRE	Lcc	RB-P	
Full Cache	26.63	32.99	49.34	42.77	27.35	18.77	32.87	24.24	27.10	71.00	86.23	42.96	2.75	86.98	55.33	52.87	42.51
B=128h																	
H2O	21.19	21.66	38.60	30.63	20.65	12.19	20.65	22.42	21.81	39.00	82.52	40.68	2.98	79.56	49.13	46.76	34.40
StreamingLLM	16.61	14.74	31.40	28.05	21.36	12.08	18.44	18.91	19.26	43.50	74.22	29.00	2.75	31.65	41.27	38.84	27.63
SnapKV	19.17	21.40	42.93	36.76	22.44	15.86	19.16	21.84	21.55	47.50	84.15	40.24	2.30	68.26	50.69	47.13	35.09
Pyramid	20.16	21.77	43.55	36.78	23.12	14.39	19.53	22.03	21.47	51.00	84.62	40.24	2.79	70.77	50.57	46.53	35.58
Ada-SnapKV	20.63	22.58	45.68	37.90	23.49	16.55	19.99	22.28	21.55	59.50	85.00	40.62	3.09	69.36	50.98	48.17	36.71
Ada-Pyramid	20.50	21.71	45.61	36.81	23.57	15.84	19.75	22.13	22.00	60.50	84.04	40.51	3.21	73.60	51.24	48.02	36.81
B=256h																	
H2O	21.54	22.92	42.56	31.07	22.53	13.76	22.52	22.40	23.09	40.50	84.20	40.77	3.41	86.10	50.98	48.17	36.03
StreamingLLM	17.93	16.01	33.36	30.71	21.30	10.08	20.66	19.47	22.89	53.50	73.59	29.22	3.00	27.77	42.30	39.87	28.85
SnapKV	22.37	23.74	48.13	38.56	22.43	15.66	21.91	23.13	23.15	61.50	85.45	41.42	3.09	84.54	53.22	50.24	38.66
Pyramid	20.09	24.00	47.33	38.24	22.48	16.02	21.40	22.45	22.63	63.00	84.93	40.98	3.40	82.48	52.78	49.36	38.22
Ada-SnapKV	22.55	25.78	48.33	40.30	24.24	16.64	21.63	23.03	23.19	67.00	85.78	41.53	3.47	87.07	53.86	51.13	39.72
Ada-Pyramid	22.64	24.64	47.40	40.25	23.62	16.83	21.82	23.34	22.70	66.50	84.99	41.34	2.78	86.90	53.17	49.52	39.28
B=512h																	
H2O	21.72	26.03	44.81	32.33	23.16	14.86	23.65	22.84	24.70	42.00	85.22	41.57	3.40	86.45	53.04	49.68	37.22
StreamingLLM	18.76	17.17	37.09	30.21	21.64	9.93	24.44	20.00	25.57	62.00	72.36	29.95	2.48	18.17	43.70	40.13	29.60
SnapKV	24.60	27.81	48.98	39.46	25.25	16.98	23.70	22.96	24.37	67.00	85.88	41.26	2.78	86.56	54.81	51.71	40.26
Pyramid	23.23	27.94	48.87	40.50	24.36	16.74	23.22	23.16	24.37	67.00	85.73	41.74	3.16	85.67	54.16	50.34	40.01
Ada-SnapKV	23.39	28.72	48.96	40.60	25.20	17.25	23.15	23.48	24.41	68.00	86.39	41.69	2.73	88.92	54.69	51.51	40.57
Ada-Pyramid	24.03	28.98	48.39	39.25	24.50	18.38	23.13	23.90	24.30	68.00	85.89	41.89	2.98	87.71	54.46	51.39	40.45
B=1024h																	
H2O	23.90	28.62	46.46	37.03	24.74	15.04	25.30	23.11	25.92	46.00	85.93	41.80	3.24	86.57	54.46	51.01	38.70
StreamingLLM	19.42	21.69	41.75	32.40	22.18	11.18	27.13	21.09	26.59	67.00	71.79	30.11	2.88	16.57	44.82	39.76	31.02
SnapKV	25.47	29.57	49.33	40.90	25.53	19.01	25.94	23.89	26.21	69.50	86.48	42.10	2.98	88.56	55.57	51.92	41.44
Pyramid	24.21	29.86	48.93	40.75	25.05	18.77	25.73	24.06	25.65	68.50	86.31	42.25	2.97	87.17	54.75	52.10	41.07
Ada-SnapKV	24.79	31.94	48.45	40.73	26.22	19.11	25.61	23.92	26.03	70.00	86.32	42.35	2.91	88.31	55.44	52.55	41.54
Ada-Pyramid	25.09	30.94	48.18	40.00	26.52	19.10	24.93	23.71	25.86	70.00	86.34	42.64	2.56	86.92	54.93	51.90	41.23

Table 1: Comparison Based on Mistral-7B-Instruct-v0.2 Among 16 Datasets

35.09 to 36.71. Similarly, Ada-Pyramid surpasses the original Pyramid in 14 of 16 datasets, boosting the average score from 35.58 to 36.81.

Figure 5 summarizes average scores of all strategies based on Mistral and LWM across 16 datasets. Overall, SnapKV and Pyramid, as the current two leading methods, exhibit closely matched performance, surpassing previous approaches such as H2O and StreamingLLM. Furthermore, our Ada-SnapKV and Ada-Pyramid strategies consistently improve the generated quality under varying budgets, especially in small budgets. The two adaptive eviction strategies alternately lead and surpass previous versions to become the new state-of-the-art methods. This consistent improvement validates the necessity and effectiveness of adaptive budget allocation, as previously demonstrated in both theoretical derivations and empirical findings.

4.3 Evaluations on Needle-in-a-Haystack Test

As shown in Figure 6, we employ a Needle-in-a-Haystack test to demonstrate how adaptive budget allocation can enhance long-context retrieval capabilities. All configurations maintain a recent window size of 32 and a pooling kernel size of 7 which is consistent with former experiments, where the maximum inference length is limited to 37K in the full cache case on A800-80G. With a cache budget of

$B = 128h$, the Ada-SnapKV and SnapKV extend the max length up to 429K, while the Ada-Pyramid and Pyramid extend to 365K. Notably, Ada-SnapKV and Ada-Pyramid both effectively improve long-text retrieval capabilities compared to previous SnapKV and Pyramid. In particular, Ada-SnapKV and Ada-Pyramid achieve near-lossless retrieval within the original 37K length, a feat not replicated by the standard SnapKV and Pyramid. In terms of average score, Ada-SnapKV improves from 94.84 to 95.99, while Ada-Pyramid increases from 96.02 to 96.69. Further details on decoding latency and maximum memory consumption during inference within varied context lengths are available in Appendix A.4.

5 Conclusion

In this study, we reexamine prevailing cache eviction strategies for efficient inference in long sequences, revealing their goal to minimize an upper bound of eviction loss, quantified as the L1 distance between pre- and post-eviction outputs. By introducing an adaptive budget allocation among various attention heads, we theoretically reduce this upper bound compared to previous methods. Our empirical findings suggest that this adaptive approach significantly benefits from the varied concentration degrees inherent in multiple heads within the self-attention mechanism. The de-

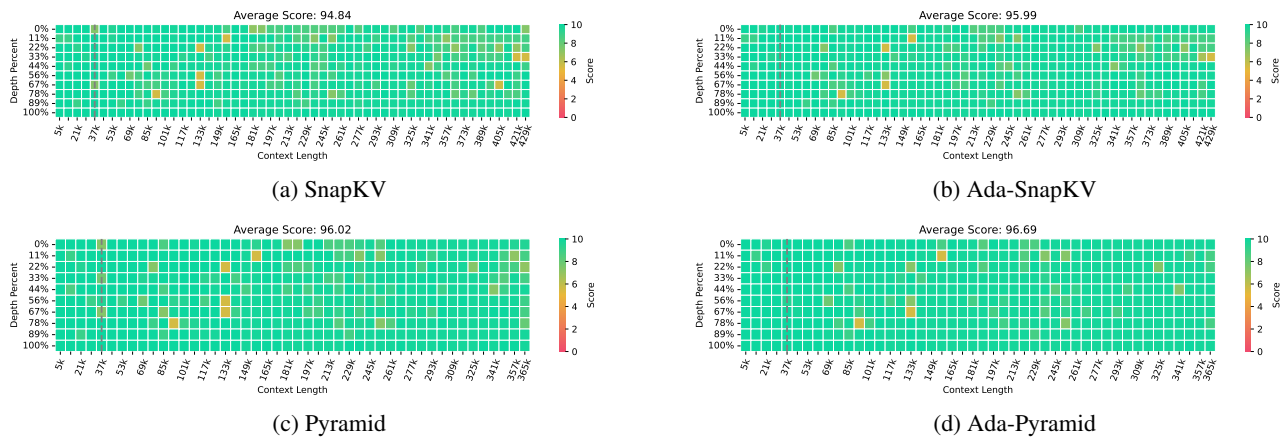


Figure 6: Needle-in-a-Haystack Test. This test inserts a critical sentence (the 'needle') within a document (the 'haystack') with extensive context, then evaluates a model's ability to retrieve the needle from the document. The x-axis indicates the context length of the document, and the y-axis shows the insertion depth of the needle. The Average Score is determined by averaging the aggregated scores at various context lengths. Higher scores indicate an improved capacity of the model for contextual retrieval.

development of two novel adaptive eviction methods, Ada-SnapKV and Ada-Pyramid, incorporating this adaptive allocation, demonstrates significant improvements in comprehensive evaluations. Furthermore, this research highlights the substantial potential for advancing cache eviction strategies through our theoretical framework and adaptive budget allocation, specifically designed to exploit the unique characteristics of different attention heads in LLMs.

References

- Achiam, J.; Adler, S.; Agarwal, S.; Ahmad, L.; Akkaya, I.; Aleman, F. L.; Almeida, D.; Altschmidt, J.; Altman, S.; Anadkat, S.; et al. 2023. Gpt-4 technical report. *arXiv preprint arXiv:2303.08774*.
- Anthropic. 2024. The claude 3 model family: Opus, sonnet, haiku. Accessed: 2024-07-09.
- Bai, Y.; Lv, X.; Zhang, J.; Lyu, H.; Tang, J.; Huang, Z.; Du, Z.; Liu, X.; Zeng, A.; Hou, L.; et al. 2023. Longbench: A bilingual, multitask benchmark for long context understanding. *arXiv preprint arXiv:2308.14508*.
- Dao, T.; Fu, D.; Ermon, S.; Rudra, A.; and Ré, C. 2022. Flashattention: Fast and memory-efficient exact attention with io-awareness. *Advances in Neural Information Processing Systems*, 35: 16344–16359.
- Dasigi, P.; Lo, K.; Beltagy, I.; Cohan, A.; Smith, N. A.; and Gardner, M. 2021. A dataset of information-seeking questions and answers anchored in research papers. *arXiv preprint arXiv:2105.03011*.
- Fabbri, A. R.; Li, I.; She, T.; Li, S.; and Radev, D. R. 2019. Multi-news: A large-scale multi-document summarization dataset and abstractive hierarchical model. *arXiv preprint arXiv:1906.01749*.
- Ge, S.; Zhang, Y.; Liu, L.; Zhang, M.; Han, J.; and Gao, J. 2023. Model tells you what to discard: Adaptive kv cache compression for llms. *arXiv preprint arXiv:2310.01801*.
- Gliwa, B.; Mochol, I.; Biesek, M.; and Wawer, A. 2019. SAMSUM corpus: A human-annotated dialogue dataset for abstractive summarization. *arXiv preprint arXiv:1911.12237*.
- Gu, Q. 2023. Llm-based code generation method for go lang compiler testing. In *Proceedings of the 31st ACM Joint European Software Engineering Conference and Symposium on the Foundations of Software Engineering*, 2201–2203.
- Guo, D.; Xu, C.; Duan, N.; Yin, J.; and McAuley, J. 2023. LongCoder: A Long-Range Pre-trained Language Model for Code Completion. *arXiv:2306.14893*.
- Ho, X.; Duong Nguyen, A.-K.; Sugawara, S.; and Aizawa, A. 2020. Constructing A Multi-hop QA Dataset for Comprehensive Evaluation of Reasoning Steps. In Scott, D.; Bel, N.; and Zong, C., eds., *Proceedings of the 28th International Conference on Computational Linguistics*, 6609–6625. Barcelona, Spain (Online): International Committee on Computational Linguistics.
- Huang, L.; Cao, S.; Parulian, N.; Ji, H.; and Wang, L. 2021. Efficient attentions for long document summarization. *arXiv preprint arXiv:2104.02112*.
- Jiang, A. Q.; Sablayrolles, A.; Mensch, A.; Bamford, C.; Chaplot, D. S.; Casas, D. d. I.; Bressand, F.; Lengyel, G.; Lample, G.; Saulnier, L.; et al. 2023. Mistral 7B. *arXiv preprint arXiv:2310.06825*.
- Joshi, M.; Choi, E.; Weld, D. S.; and Zettlemoyer, L. 2017. TriviaQA: A Large Scale Distantly Supervised Challenge Dataset for Reading Comprehension. *arXiv:1705.03551*.
- Kočiský, T.; Schwarz, J.; Blunsom, P.; Dyer, C.; Hermann, K. M.; Melis, G.; and Grefenstette, E. 2018. The narrativeqa reading comprehension challenge. *Transactions of the Association for Computational Linguistics*, 6: 317–328.
- Kwon, W.; Li, Z.; Zhuang, S.; Sheng, Y.; Zheng, L.; Yu, C. H.; Gonzalez, J.; Zhang, H.; and Stoica, I. 2023. Efficient memory management for large language model serving with

- pagedattention. In *Proceedings of the 29th Symposium on Operating Systems Principles*, 611–626.
- Laban, P.; Kryściński, W.; Agarwal, D.; Fabbri, A. R.; Xiong, C.; Joty, S.; and Wu, C.-S. 2023. SUMMEDITs: measuring LLM ability at factual reasoning through the lens of summarization. In *Proceedings of the 2023 Conference on Empirical Methods in Natural Language Processing*, 9662–9676.
- Li, X.; and Roth, D. 2002. Learning question classifiers. In *COLING 2002: The 19th International Conference on Computational Linguistics*.
- Li, Y.; Huang, Y.; Yang, B.; Venkitesh, B.; Locatelli, A.; Ye, H.; Cai, T.; Lewis, P.; and Chen, D. 2024. Snapkv: Llm knows what you are looking for before generation. *arXiv preprint arXiv:2404.14469*.
- Liu, H.; Yan, W.; Zaharia, M.; and Abbeel, P. 2024. World model on million-length video and language with ringattention. *arXiv preprint arXiv:2402.08268*.
- Liu, T.; Xu, C.; and McAuley, J. 2023. RepoBench: Benchmarking Repository-Level Code Auto-Completion Systems. *arXiv:2306.03091*.
- Liu, Z.; Wang, J.; Dao, T.; Zhou, T.; Yuan, B.; Song, Z.; Shrivastava, A.; Zhang, C.; Tian, Y.; Re, C.; and Chen, B. 2023. DeJa Vu: Contextual Sparsity for Efficient LLMs at Inference Time. *arXiv:2310.17157*.
- Reid, M.; Savinov, N.; Teplyashin, D.; Lepikhin, D.; Lillcrap, T.; Alayrac, J.-b.; Soricut, R.; Lazaridou, A.; Firat, O.; Schrittwieser, J.; et al. 2024. Gemini 1.5: Unlocking multimodal understanding across millions of tokens of context. *arXiv preprint arXiv:2403.05530*.
- Sun, H.; Chen, Z.; Yang, X.; Tian, Y.; and Chen, B. 2024. Triforce: Lossless acceleration of long sequence generation with hierarchical speculative decoding. *arXiv preprint arXiv:2404.11912*.
- Tang, J.; Zhao, Y.; Zhu, K.; Xiao, G.; Kasikci, B.; and Han, S. 2024. Quest: Query-Aware Sparsity for Efficient Long-Context LLM Inference. *arXiv preprint arXiv:2406.10774*.
- Trivedi, H.; Balasubramanian, N.; Khot, T.; and Sabharwal, A. 2022. MuSiQue: Multihop Questions via Single-hop Question Composition. *Transactions of the Association for Computational Linguistics*, 10: 539–554.
- Wang, K.; and Chen, F. 2023. Catalyst: Optimizing Cache Management for Large In-memory Key-value Systems. *Proceedings of the VLDB Endowment*, 16(13): 4339–4352.
- Xiao, G.; Tian, Y.; Chen, B.; Han, S.; and Lewis, M. 2023. Efficient streaming language models with attention sinks. *arXiv preprint arXiv:2309.17453*.
- Yang, D.; Han, X.; Gao, Y.; Hu, Y.; Zhang, S.; and Zhao, H. 2024. PyramidInfer: Pyramid KV Cache Compression for High-throughput LLM Inference. *arXiv preprint arXiv:2405.12532*.
- Yang, Z.; Qi, P.; Zhang, S.; Bengio, Y.; Cohen, W. W.; Salakhutdinov, R.; and Manning, C. D. 2018. HotpotQA: A dataset for diverse, explainable multi-hop question answering. *arXiv preprint arXiv:1809.09600*.
- Yi, Z.; Ouyang, J.; Liu, Y.; Liao, T.; Xu, Z.; and Shen, Y. 2024. A Survey on Recent Advances in LLM-Based Multi-turn Dialogue Systems. *arXiv preprint arXiv:2402.18013*.
- Zhang, Y.; Gao, B.; Liu, T.; Lu, K.; Xiong, W.; Dong, Y.; Chang, B.; Hu, J.; Xiao, W.; et al. 2024a. PyramidKV: Dynamic KV Cache Compression based on Pyramidal Information Funneling. *arXiv preprint arXiv:2406.02069*.
- Zhang, Z.; Sheng, Y.; Zhou, T.; Chen, T.; Zheng, L.; Cai, R.; Song, Z.; Tian, Y.; Ré, C.; Barrett, C.; et al. 2024b. H2o: Heavy-hitter oracle for efficient generative inference of large language models. *Advances in Neural Information Processing Systems*, 36.
- Zhong, M.; Yin, D.; Yu, T.; Zaidi, A.; Mutuma, M.; Jha, R.; Awadallah, A. H.; Celikyilmaz, A.; Liu, Y.; Qiu, X.; et al. 2021. QMSum: A new benchmark for query-based multi-domain meeting summarization. *arXiv preprint arXiv:2104.05938*.

A Appendix

A.1 Proof of Theorem 1

Theorem. *The post-eviction output o' can rewrite as:*

$$o' = \sum_{i \in [h]} \frac{A_i \odot \mathcal{N}_i}{\|A_i \odot \mathcal{N}_i\|_1} V_i W_i^O \quad (15)$$

$$\text{where } \mathcal{N}_i^j = \begin{cases} 1 & \text{if } K_i^j \text{ and } V_i^j \text{ are retained} \\ 0 & \text{otherwise, evict } K_i^j \text{ and } V_i^j \end{cases}$$

and \odot indicates element-wise multiplication

$$\text{given budget allocation } \{B_i\} \text{ s.t. } \sum_{i \in [h]} B_i = B$$

Proof. Consider the softmax function as:

$$\text{softmax}(x) = \frac{\exp(x^j)}{\sum^j \exp(x^j)} \quad (16)$$

Thus, the attention weight after eviction procedure is:

$$A'_i = \text{softmax}(s_i + \mathcal{M}_i) \text{ where } s_i = q_i K_i^T \quad (17)$$

$$A'_i = \frac{\exp(s_i^j + \mathcal{M}_i^j)}{\sum^j \exp(s_i^j + \mathcal{M}_i^j)} = \frac{\exp(s_i^j) \odot \mathcal{N}_i^j}{\sum^j \exp(s_i^j) \odot \mathcal{N}_i^j} \quad (18)$$

$$= \frac{\exp(s_i^j) \odot \mathcal{N}_i^j}{\sum^j \exp(s_i^j)} \frac{\sum^j \exp(s_i^j)}{\sum^j \exp(s_i^j) \odot \mathcal{N}_i^j} \quad (19)$$

$$= \frac{A_i \odot \mathcal{N}_i}{\|A_i \odot \mathcal{N}_i\|_1} \quad (20)$$

$$\text{where } \mathcal{N}_i^j = \begin{cases} 1 & \text{if } K_i^j \text{ and } V_i^j \text{ are retained} \\ 0 & \text{otherwise, evict } K_i^j \text{ and } V_i^j \end{cases} \quad (21)$$

Thus:

$$o' = \sum_{i \in [h]} A'_i V_i W_i^O = \sum_{i \in [h]} \frac{A_i \odot \mathcal{N}_i}{\|A_i \odot \mathcal{N}_i\|_1} V_i W_i^O \quad (22)$$

$$\text{where } \mathcal{N}_i^j = \begin{cases} 1 & \text{if } K_i^j \text{ and } V_i^j \text{ are retained} \\ 0 & \text{otherwise, evict } K_i^j \text{ and } V_i^j \end{cases}$$

$$\text{given budget allocation } \{B_i\} \text{ s.t. } \sum_{i \in [h]} B_i = B$$

□

A.2 Proof of Theorem 2

Theorem. *The eviction loss caused by cache eviction can be bounded by D as follows:*

$$\text{Eviction Loss} \leq D = 2hC - 2C \sum_{i \in [h] \text{ retained}} \sum_{i \in [h]} A_i^j \quad (23)$$

$$\text{given budget allocation } \{B_i\} \text{ s.t. } \sum_{i \in [h]} B_i = B$$

where $C = \text{Max} \{\|V_i W_i^O\|_1\}$ is the max value in the L1-norm of Matrices $\{V_i W_i^O\}$ among all head.

Proof. By calculating the L1 distance between their outputs, we can obtain

$$\|o' - o\|_1 = \left\| \sum_{i \in [h]} \left(\mathbf{1} - \frac{\mathcal{N}_i}{\|A_i \odot \mathcal{N}_i\|_1} \right) \odot A_i V_i W_i^O \right\|_1 \quad (24)$$

$$\leq \sum_{i \in [h]} \left\| \left(\mathbf{1} - \frac{\mathcal{N}_i}{\|A_i \odot \mathcal{N}_i\|_1} \right) \odot A_i V_i W_i^O \right\|_1 \quad (25)$$

$$\leq \sum_{i \in [h]} \left\| \left(\mathbf{1} - \frac{\mathcal{N}_i}{\|A_i \odot \mathcal{N}_i\|_1} \right) \odot A_i \right\|_1 \|V_i W_i^O\|_\infty \quad (26)$$

$$\leq C \sum_{i \in [h]} \left\| \left(\mathbf{1} - \frac{\mathcal{N}_i}{\|A_i \odot \mathcal{N}_i\|_1} \right) \odot A_i \right\|_1 \quad (27)$$

$$\text{where } C = \text{Max} \left\{ \|V_i W_i^O\|_\infty \right\}$$

By expanding A_i , we can further simplify the expression.

$$\|o' - o\|_1 \leq C \sum_{i \in [h]} \sum_{\text{retained } j} \left(\frac{A_i^j}{\sum_{\text{retained } j} A_i^j} - A_i^j \right) + \sum_{\text{evicted } j} A_i^j \quad (28)$$

$$= C \sum_{i \in [h]} \sum_{\text{retained } j} \left(\frac{A_i^j}{\sum_{\text{retained } j} A_i^j} \right) - \sum_{\text{retained } j} A_i^j + \sum_{\text{evicted } j} A_i^j \quad (29)$$

$$= C \sum_{i \in [h]} \left(2 - 2 \sum_{\text{retained } j} A_i^j \right) \quad (30)$$

$$= 2hC - 2C \sum_{i \in [h]} \sum_{\text{retained } j} A_i^j \quad (31)$$

□

A.3 Proof of Theorem 4

Theorem. *The upper bound D'' of eviction loss with adaptive budget allocation consistently remains at or below the upper bound D' associated with uniform allocation.*

$$D'' \leq D' \quad (32)$$

Proof.

$$D' = 2hC - 2C \sum_{i \in [h]} \sum_{\substack{j \in [n] \\ A_i^j \in \text{Top-K}(A_i, B_i)}} A_i^j \quad (33)$$

given uniform allocation $\{B_i = B/h\}$

$$D'' = 2hC - 2C \sum_{i \in [h]} \sum_{\substack{j \in [n] \\ A_i^j \in \text{Top-K}(A_i, B_i^*)}} A_i^j \quad (34)$$

given adaptive allocation $\{B_i = B_i^*\}$

Based on the operations of concatenation and Top-K in the first and second lines of Algorithm 2, we can flatten the second \sum in D'' as follow:

$$D'' = 2hC - 2C \sum_{\substack{i \in [h], j \in [n] \\ A_i^j \in \text{Top-K}(A, B)}} A_i^j \quad (35)$$

$$\text{where } B = \sum_i B_i^* = \sum_i B_i$$

Considering that $B = \sum B_i = \sum B_i^*$, it is evident that $\sum_{\substack{i \in [h], j \in [n] \\ A_i^j \in \text{Top-K}(A, B)}} A_i^j \geq \sum_{i \in [h]} \sum_{\substack{j \in [n] \\ A_i^j \in \text{Top-K}(A_i, B_i)}} A_i^j$. This is because under the premise of identical total budget, the global Top-K sum is greater than or equal to the sum of local Top-K sums of each head. Thus:

$$D'' \leq D' \quad (36)$$

□

	Single-Doc. QA			Multi-Doc. QA			Summarization			Few-shot Learning			Synthetic		Code		Ave. Score
	NrtvQA	Qasper	MF-en	HotpotQA	2WikiMQA	Musique	GovReport	QMSum	MultiNews	TREC	TriviaQA	SAMSum	PCount	PRE	Lcc	RB-P	
Full Cache	18.00	25.80	43.10	23.40	16.70	9.70	27.20	25.00	24.70	70.50	61.60	39.60	3.00	6.50	42.20	41.60	29.91
B=128h																	
H2O	17.90	17.73	36.10	21.52	17.51	9.26	16.13	22.99	19.64	43.50	60.64	36.36	3.00	5.50	34.93	36.74	24.97
StreamingLLM	12.81	11.32	29.04	17.24	13.67	6.91	16.34	20.25	17.35	41.00	52.74	25.77	0.50	3.00	28.38	30.98	20.46
SnapKV	17.51	17.57	38.89	22.15	17.28	9.13	15.01	21.96	17.94	46.00	61.05	35.97	0.00	4.00	36.92	37.83	24.95
Pyramid	18.17	17.58	39.08	22.05	16.78	8.13	14.74	22.24	17.88	47.50	60.11	37.02	0.50	3.50	36.96	38.73	25.06
Ada-SnapKV	18.64	18.61	39.59	22.51	17.05	9.19	15.28	22.88	18.98	52.50	61.69	36.76	0.00	3.00	36.82	39.63	25.82
Ada-Pyramid	18.35	18.93	39.49	22.57	16.83	8.61	15.05	23.22	18.85	55.50	60.93	37.39	0.50	3.50	36.55	39.79	26.00
B=256h																	
H2O	18.99	19.18	38.78	21.88	17.33	9.16	16.88	23.29	20.51	48.00	60.36	38.07	3.00	5.50	37.18	37.94	26.00
StreamingLLM	13.59	11.81	29.73	18.59	14.37	6.72	21.06	20.78	21.29	51.50	51.92	26.51	0.50	3.00	28.97	31.09	21.96
SnapKV	19.27	20.61	40.78	22.81	16.83	9.89	16.23	23.17	20.07	53.50	61.75	38.41	0.00	4.00	38.25	40.57	26.63
Pyramid	18.81	19.83	40.71	22.34	17.10	9.08	16.10	22.93	19.50	60.00	61.01	38.65	0.50	5.00	38.23	39.13	26.81
Ada-SnapKV	18.99	21.08	41.18	22.89	17.64	9.52	16.71	23.05	20.48	67.00	61.27	38.74	0.00	3.50	39.60	40.96	27.66
Ada-Pyramid	18.78	20.32	40.50	22.73	17.01	9.37	16.05	23.60	19.93	69.00	61.43	39.07	2.00	5.00	38.40	40.08	27.70
B=512h																	
H2O	18.61	20.07	39.82	22.08	17.21	10.13	17.62	23.65	21.41	54.50	61.84	38.74	3.00	5.50	39.23	40.08	27.09
StreamingLLM	13.94	13.13	33.06	18.26	14.44	7.41	25.24	21.00	23.78	60.50	52.04	26.31	1.00	3.00	30.10	31.76	23.44
SnapKV	18.45	21.96	42.01	23.25	17.42	9.88	17.68	23.62	21.30	68.00	61.77	39.02	1.00	4.50	40.09	40.79	28.17
Pyramid	18.46	22.85	42.24	23.27	16.75	9.45	17.41	24.62	21.20	70.00	60.61	39.32	3.00	6.50	39.63	40.78	28.51
Ada-SnapKV	18.83	22.39	42.15	23.52	18.27	9.63	17.66	23.99	21.23	70.00	61.72	38.93	2.00	4.50	40.11	41.28	28.51
Ada-Pyramid	18.64	22.86	41.81	23.61	16.67	9.45	17.35	23.75	20.79	70.00	60.66	39.61	3.00	5.50	39.87	40.99	28.41
B=1024h																	
H2O	17.11	22.34	41.26	22.09	17.47	9.60	18.82	23.94	22.49	61.00	62.33	38.68	3.00	5.50	41.23	41.18	28.00
StreamingLLM	14.78	16.77	37.64	18.77	14.63	7.39	26.43	21.47	24.21	67.00	53.00	25.99	0.50	3.00	31.51	32.31	24.71
SnapKV	18.45	24.18	42.50	23.53	17.32	10.23	19.00	24.26	23.04	69.50	62.22	39.88	3.00	5.50	41.15	41.91	29.10
Pyramid	18.48	24.87	42.11	23.45	16.97	9.84	18.93	24.50	22.77	69.50	61.65	39.73	2.50	5.00	41.07	41.27	28.91
Ada-SnapKV	18.94	23.68	43.27	23.28	17.15	9.89	18.58	23.46	22.65	70.00	62.24	39.83	2.50	5.50	41.68	42.88	29.10
Ada-Pyramid	19.00	23.83	43.36	23.48	17.03	9.32	18.70	24.11	22.61	69.50	61.83	39.75	2.50	6.00	40.85	41.80	28.98

Table 2: Comparison Based on LWM-Text-Chat-1M Among 16 Datasets

A.4 Computational Efficiency

We assess the computational efficiency of Ada-SnapKV and Ada-Pyramid under adaptive allocation, as well as the original versions of SnapKV and Pyramid, using a budget of 128h across various context lengths within needle-in-a-haystack test. As shown in Figure 7, the peak memory footprint during inference for Ada-SnapKV and Ada-Pyramid, as well as SnapKV and Pyramid, remains almost consistent as sequence length increases, significantly lower than that of vanilla Full Cache. Consequently, this allows the original sequence length of 37K to be extended to most 429K, achieving a 10.59-fold improvement. In terms of speed, as shown in 8, the decoding latency of the four strategies remains almost consistent and is independent of the context length, which is significantly lower than the decoding latency under Full Cache. This is primarily due to cache eviction, which greatly reduces the size of the KV Cache, thereby significantly alleviating the IO latency bottleneck in the autoregressive decoding stage.

A.5 Detailed results for LWM model Among 16 Datasets

The table 2 presents quality scores of different eviction strategies based on the LWM model across 16 datasets. Overall, the results are consistent with those of Mistral, and the adaptive allocation also leads to quality improvements after cache eviction.

A.6 Detailed Information of Datasets

Table 3 provides a comprehensive description of information pertaining to 16 datasets.

A.7 Detailed Visualization of Head Concentration

Figure 9 supplements Figure 3 in the main paper by presenting the visualization results across all layers. It can be observed that in all layers, different heads exhibit significant variations in attention concentration. This indicates that the adaptive allocation algorithm has great potential to reduce the eviction loss in practice.

A.8 Code

We are in the process of making our source code available to the public.

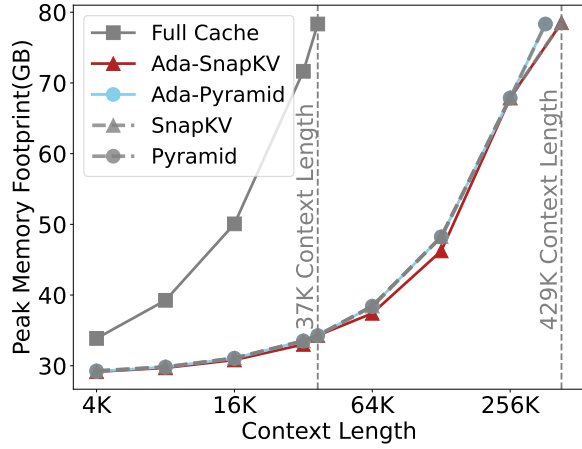


Figure 7: Peak Memory Footprint

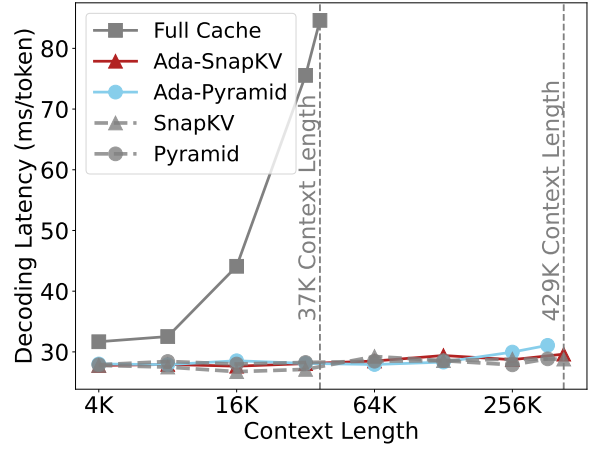


Figure 8: Decoding Latency

Label	Task	Task Type	Eval metric	Avg len	Language	Sample Num
NrtvQA	NarrativeQA	Single-Doc. QA	F1	18,409	EN	200
Qasper	Qasper	Single-Doc. QA	F1	3,619	EN	200
MF-en	MultiFieldQA-en	Single-Doc. QA	F1	4,559	EN	150
HotpotQA	HotpotQA	Multi-Doc. QA	F1	9,151	EN	200
2WikiMQA	2WikiMultihopQA	Multi-Doc. QA	F1	4,887	EN	200
Musique	MuSiQue	Multi-Doc. QA	F1	11,214	EN	200
GovReport	GovReport	Summarization	Rouge-L	8,734	EN	200
QMSum	QMSum	Summarization	Rouge-L	10,614	EN	200
MultiNews	MultiNews	Summarization	Rouge-L	2,113	EN	200
TREC	TREC	Few-shotLearning	Accuracy	5,177	EN	200
TriviaQA	TriviaQA	Few-shotLearning	F1	8,209	EN	200
SAMSum	SAMSum	Few-shotLearning	Rouge-L	6,258	EN	200
PCount	PassageCount	Synthetic	Accuracy	11,141	EN	200
PRe	PassageRetrieval-en	Synthetic	Accuracy	9,289	EN	200
Lcc	LCC	Code	Edit Sim	1,235	Python/C#/Java	500
RB-P	RepoBench-P	Code	Edit Sim	4,206	Python/Java	500

Table 3: Details of 16 Datasets

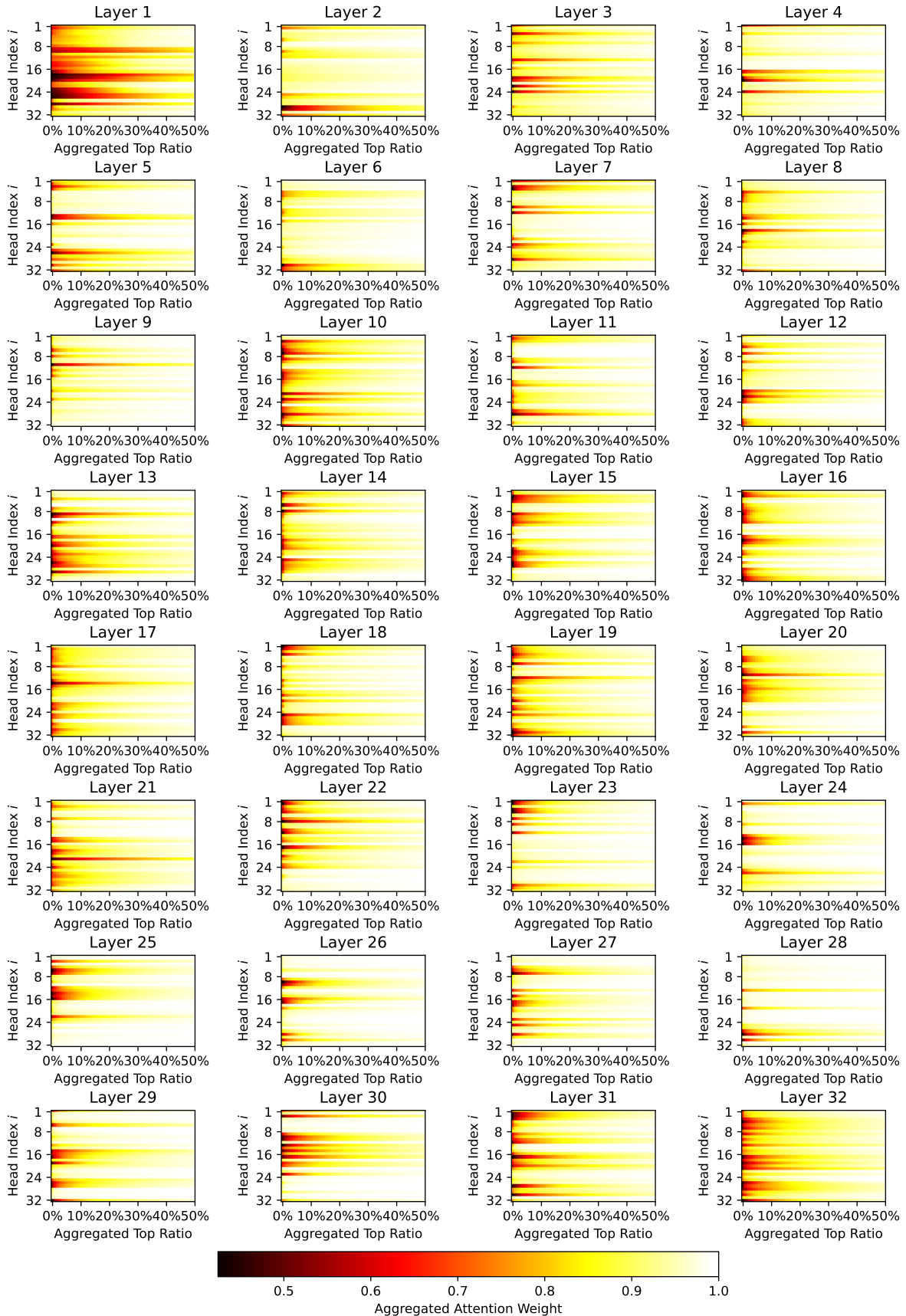


Figure 9: Visualization of Heads' Concentrations